

REAL-TIME LOCALIZATION OF AN UNMANNED GROUND VEHICLE USING A 360 DEGREE RANGE SENSOR

Soon-Yong Park and Sung-In Choi

School of Computer Science and Engineering, Kyungpook National University
1370 Sankyuk-dong, Puk-gu, Daegu, 702-701 Korea

Keywords: Localization, 3D Sensor, Registration, Unmanned vehicle.

Abstract: A computer vision technique for the localization of an unmanned ground vehicle (UGV) is presented. The proposed technique is based on 3D registration of a sequence of 360 degree range data and a digital surface model (DSM). 3D registration of a sequence of dense range data requires a large computation time. For real time localization, we propose projection-based registration and uniform arc length sampling (UALS) techniques. UALS reduces the number of 3D sample points while maintaining their uniformity over range data in terms of ground sample distance. The projection-based registration technique reduces the time of 3D correspondence search. Experimental results from two real navigation paths are shown to verify the performance of the proposed method.

1 INTRODUCTION

Three dimensional (3D) registration is a computer vision technique to align multi-view range data with respect to a common coordinate system. Many investigations have been introduced for 3D model reconstruction, 3D robot vision, etc. Recently in robotics community, 3D registration is applied to localization of unmanned robots or vehicles from range data acquired from 3D sensors.

A 3D sensor mounted on an unmanned vehicle captures the 3D shape around the vehicle, which is a local 3D map represented with respect to the sensor coordinate system. If there is a global and reference 3D map which contains the 3D shape information of navigation environment, the vehicle location can be determined by matching the local map with respect to the global map. By the way, an initial position of the vehicle can be coarsely estimated by a GPS or INS sensor. Therefore, it only needs to refine the initial position to correctly match local and global 3D maps.

A common approach of 3D registration is using the ICP algorithm (Besl and McKay., 1992). R. Madhavan *et al.* (Madhavan *et al.*, 2005) register a sequence of 3D range data in a pair-wise manner to determine a robot pose. A modified ICP algorithm is employed to cope with matching outliers. Triebel *et al.* (Triebel *et al.*, 2006) introduce multi-level surface maps to classify surface patches to several object cat-

egories. Levinson *et al.* (Levinson *et al.*, 2007) use a digital map of urban environment. A particle filter is used to match local range data to the map.

In a few investigations, 360 degree range sensors are used to capture omnidirectional range data. Himmelsbach *et al.* (Himmelsbach *et al.*, 2008) segment, classify, and track 3D objects using a 360 degree laser sensor. They generate occupancy grids from range data to identify obstacles. Kümmerle *et al.* (Kümmerle *et al.*, 2009) present an autonomous driving technique of an unmanned vehicle which is equipped with multiple navigation sensors including a 360 degree range sensor. In our previous work, a 3D registration technique is introduced to align 360 degree range data and a digital surface model (DSM)(Park and Choi, 2009).

Matching 3D maps obtained from different coordinate systems requires a reasonable number of correspondences between the maps (Hartley and Zisserman, 2000). Since a 360 degree range sensor captures a huge number of 3D points, it requires a significant time for 3D registration. For real-time localization of an unmanned ground vehicle (UGV), we introduce projection-based registration and uniform ground distance sampling techniques to reduce the number of correspondence. Experimental results show that the proposed method can find robot position in about 15Hz rate.

2 RANGE FORMAT & SAMPLING

2.1 Range Data Format

The range sensor used in this paper is a Velodyne HDL-64ES2 LADAR sensor mounted on the top of an UGV. The sensor captures 360 degree range data by rotating 64 lasers and detectors at 10Hz revolution rate. The sensor is mounted at 2.081m height from the ground. The vertical field of view of the sensor is 26.8 degree, 2 degree above and 24.2 degree below the horizontal plane.

Each laser detector captures maximum 2048 3D points in a single revolution. Total 64 laser detectors then capture 3D point clouds which are represented with respect to the sensor coordinate system as shown in Figure 1. To rasterize the 3-D data, we convert the point clouds to a 2.5D depth map called ‘‘range frame’’. The size of the map is 64×1800 in row and column, where the row index L and the column index ϕ correspond to the laser number and the horizontal angle, respectively. As the column index, 360 degree range data is quantized with 0.2 degree angular resolution.

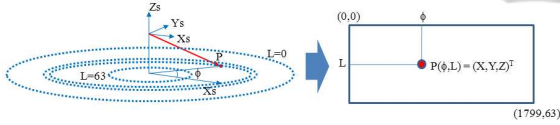


Figure 1: Format of 360 degree range frame.

2.2 Uniform Arc Length Sampling

In this section, we propose a new sampling method called a uniform arc length sampling (UALS) technique. In contrast to conventional uniform point sampling (UPS) techniques, our approach uniformly samples 3D points in terms of ground distance along the scan circles. Let $\alpha(L)$ be the circumference of a scanning circle of a line L , and $\theta(L)$ be a vertical angle between the horizontal plane and a ray from the sensor to line L . Then $\alpha(L)$ is proportional to the $\tan(90 - \theta(L))$.

If $\theta(L)$ is larger than 1.0 degree, $\alpha(L)$ is computed as shown in Equation 1. In this equation, h is the height of the sensor from the ground, d_{max} is the maximum sensing distance, and α_{max} is the maximum circumference. The sampling interval $\phi_s(L)$ along the rotation angle is then computed by dividing the maximum sensing circumference by $\alpha(L)$ as in Equation 2.

$$\alpha(L) = \begin{cases} \alpha_{max} = 2\pi d_{max} & \text{if } \theta > 1.0, \\ 2\pi h \times \tan(90 - \theta(L)) & \text{otherwise.} \end{cases} \quad (1)$$

$$\phi_s(L) = \lfloor \frac{k\alpha_{max}}{\alpha(L)} + 0.5 \rfloor \quad (2)$$

In each scanning line of a range frame, we sample 3D points from the first point $P(0, L)$ to the i -th sample point such that

$$P_i(L) = P(i \times \phi_s(L), L). \quad (3)$$

As shown in the right of Figure 2, sampling is done with uniform arc length $k\alpha_{max}$ regardless of scanning distance of each line. Here, k is a constant to control the density of sampled points. However, in conventional UPS method, $\phi_s(L)$ is constant. Depending on the value of $\phi_s(L)$, the sampling density could be too dense or sparse in UPS method. On the contrary, UALS method samples 3D points uniformly over all scanning lines in terms of ground sample distance.

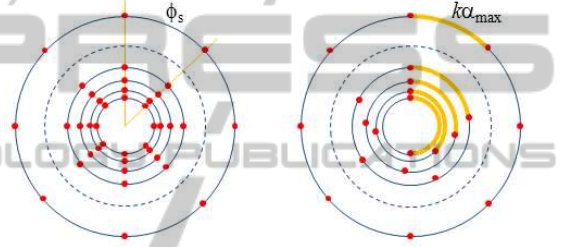


Figure 2: Comparison of two sampling methods, UPS and UALS.

3 AUTOMATIC LOCALIZATION

3.1 Localization Scheme

Localization of an UGV is done by two separate registration steps as shown in Figure 3. A pairwise (local) registration step is followed by a (global) registration step. The local registration aligns two consecutive range frames and computes the transformation of the current range frame with respect to an initial position. However, accumulation errors due to the registration of a long sequence of range data could yield erroneous localization. To overcome this problem, a global registration is done next (Park and Choi, 2009).

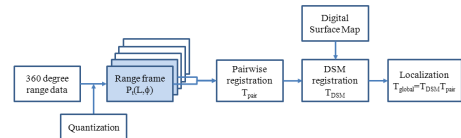


Figure 3: Flow of autonomous localization.

3.2 Projection-based ICP

In pair-wise registration, it is required to find corre-

spondences between two 3D range frames, source and destination as shown in Figure 4. Suppose there is a 3D point \mathbf{P} in the source frame. Then, we need to find a matching point \mathbf{Q}' in the destination. A projection-based registration is introduced for fast correspondence search.

Suppose the source is the current frame (n) and the destination is the previous frame ($n-1$). The previous frame is considered to be aligned already with respect to a reference coordinate system. Let the current position of the source frame be the same with that of the destination, which is $\mathbf{T}_{n-1,0}$. To find the correspondence, we first transform the source point \mathbf{P} to the initial position such that $\mathbf{P}' = \mathbf{T}_{n-1,0}^{-1}\mathbf{P}$. Second, \mathbf{P}' is projected to a 2D point $q(\phi, L)$ in the destination frame by calculating ϕ and L . Then, we search \mathbf{Q} which is the closest to \mathbf{P} . Since two range frames are reasonably close enough, we can restrict the search range as shown in the figure. In real experiments, we fix the angle search range to $\pm 15^\circ$ and the line range to ± 3 from $q(\phi, L)$.

The corresponding point \mathbf{Q}' is now derived as the intersection of the normal vector of \mathbf{P} with the tangent plane at \mathbf{Q} . After a sufficient number of correspondences are defined, a transformation matrix $\mathbf{T}_{pair} = [\mathbf{R}_{pair} | \mathbf{t}_{pair}]$ can be derived to minimize the registration error ϵ_{pair} as in Equation 4.

$$\epsilon_{pair} = \sum_{k=1}^K \|\mathbf{Q}'_k - (\mathbf{R}_{pair}\mathbf{P}_k + \mathbf{t}_{pair})\|^2. \quad (4)$$

After the pair-wise registration is finished, the position of the current frame is refined using a digital surface model. An ICP-based method is used in the second step. However, the DSM is divided into multiple elevation layers to speed up the global registration (Park and Choi, 2009).

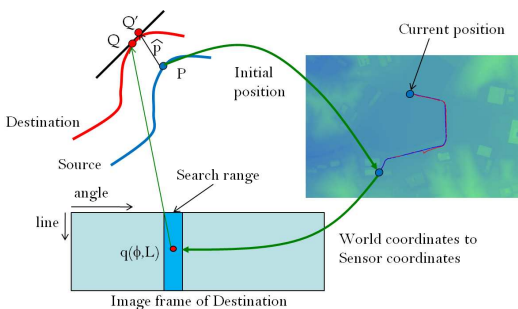


Figure 4: Projection-based pairwise registration scheme.

4 EXPERIMENTAL RESULTS

To analyze the localization error of the proposed method, two different navigation paths are used.

Along each navigation path, we drive an outdoor UGV and acquire a sequence of 3D range data. At the same time, we record the ground truth positions of the path in every revolution of the 360 degree range sensor. The sensor is rotated in 10Hz revolution speed. The UGV used in this experiment is shown in Figure 5(a). A DSM with two navigation regions is shown in Figure 5(b). Table 1 shows some properties of two navigation paths.

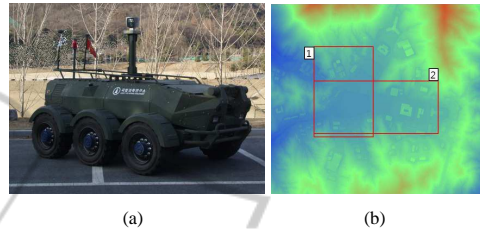


Figure 5: (a) An UGV with 360 degree range sensor (b) DSM.

Table 1: Properties of navigation paths.

Path	Path-1	Path-2
# of frames	650	970
DSM size(pixel)	969×2713	1677×1441
DSM accuracy (m)	0.5	0.5

We compare our localization method with an ICP algorithm. In this ICP algorithm, source points are sampled by UPS and the k-d tree search algorithm is also combined when searching the closest points. In each navigation path, average registration error and processing time are recorded. For fair comparison, the number of sampled points of two methods are set as same as possible.

Table 2 shows the results of two paths. In both paths, localization time of our method is less than 0.1sec, which means more than 10Hz speed. Localization speed is about three times faster than the ICP method. Localization error is also smaller than the ICP.

Table 2: Average localization error and time.

Path	Method	Error (m)	Time (msec)
Path-1	ICP+UPS	6.5	273.9
	Proposed	4.63	92.4
Path-2	ICP+UPS	7.27	365.3
	Proposed	4.46	97.3

Figure 6 plots the vehicle positions of two experiments with respect to the ground truth. In each figure, our method is compared with the ICP method. Plots of our method are closer to the ground truth. Figure 7 shows localization error in each frame of the test sequences. Compare to the ICP method, our method

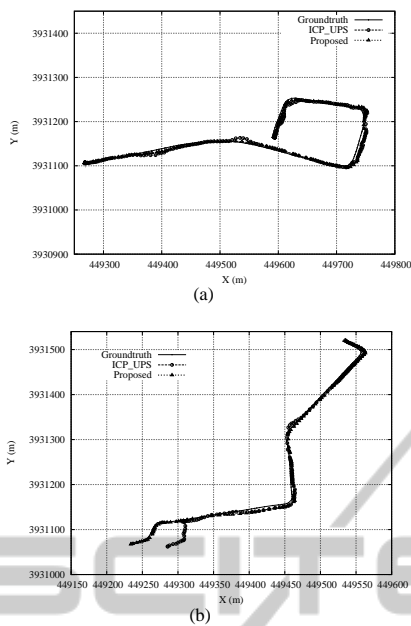


Figure 6: Localization path comparison (a)Path-1 (b)Path-2.

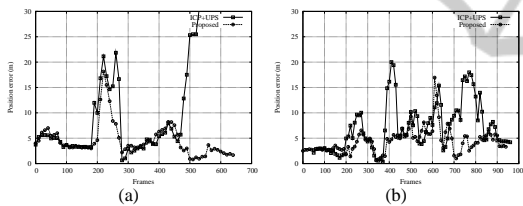


Figure 7: Localization error in the test sequences (a)Path-1 (b)Path-2.

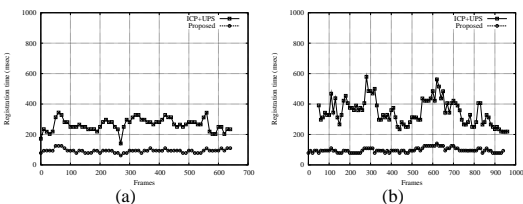


Figure 8: Localization time in the test sequences (a)path-1 (b)path-2.

yields smaller localization error through all frames. Figure 8 compares localization time of two methods. There shows high variance in the ICP method, which means unstable localization. On the contrary, localization of our method is very fast and stable.

5 CONCLUSIONS

Real time localization of an unmanned ground vehicle is introduced. A pairwise registration of 360 de-

gree range data is implemented through a projection-based iterative alignment. Without searching matching points in 3-D space, the projection-based method can find correspondences in very fast time. To reduce the number of matching pairs as small as possible, a uniform arc length sampling method is also proposed. Using the proposed sampling method, matching pairs are uniformly distributed in terms of ground distance between samples. Experiments are done using sequences of 3D range data obtained from two navigation paths. In terms of speed and accuracy, the proposed method yield better performance than a conventional method.

ACKNOWLEDGEMENTS

The Authors gratefully acknowledge the supports in part from UTRC(Unmanned technology Research Center) at KAIST, originally funded by DAPA, ADD and MKE under the Core Technology Development for Breakthrough of Robot Vision Research support program supervised by the NIPA (NIPA-2010-C7000-1001-0006).

REFERENCES

Besl, P. J. and McKay., N. D. (1992). A method for registration of 3-d shapes. *IEEE Trans. on Pattern Recognition and Machine Intelligence*, 14(2):239-256.

Hartley, R. I. and Zisserman, A. (2000). *Multiple View Geometry in Computer Vision*. Cambridge University Press.

Himmelsbach, M., Muller, A., Luttel, T., and Wunsche, H. (2008). Lidar- based 3d object perception. In *Proc. of the 1st Int'l Workshop on Cognition for Technical Systems*.

Kummerle, R., Hahnel, D., Dolgov, D., Thrun, S., and Burgard, W. (2009). Autonomous driving in a multi-level parking structure. In *Proc. of the IEEE Int'l Conf. on Robotics and Automation*.

Levinson, J., Montemerlo, M., and Thrun, S. (2007). Map-based precision vehicle localization in urban environments. In *Proc. of Robotics: Science and Systems*.

Madhavan, R., Hong, T., and Messina, E. (2005). Temporal range registration for unmanned ground and aerial vehicles. *Journal of Intelligent and Robotic Systems*, 44(1):47-69.

Park, S. and Choi, S. I. (2009). Localization of an unmanned ground vehicle using 3d registration of laser range data and dsm. In *Workshop of Applications of Computer Vision*.

Triebel, R., Pfaff, P., and Burgard, W. (2006). Multi-level surface maps for outdoor terrain mapping and loop closing. In *Int'l Conf. on Intelligence Robotics and Systems(IROS)*, pages 2276-2282.